JJEE
Volume X | Number X | Month 20XX | Pages XXX-XXX

Jordan Journal of Electrical Engineering

ISSN (print): 2409-9600, ISSN (online): 2409-9619

Homepage: jjee.ttu.edu.jo

Model-Based Theoretical Prediction of the Electric Field Dependence of the Diffusion Coefficients of Various Semiconductor Wires

Yasuhisa Omura[1, 2*]

[1] Organization for Research and Development of Innovative Science and Technology, Kansai University, Suita, Osaka, Japan

[2] Academic Collaboration Associates, Kanagawa, Japan

E-mail: omuray@kansai-u.ac.jp

Received: Mar 26, 2024 *Revised: May 03, 2024* *Accepted: May 07, 2024* *Available online: Sep 15, 2024*

***Abstract*—** This paper investigates how the diffusion coefficients of various semiconductor wires - namely Si, Ge, and 4H-SiC - are modulated by an external electric field assuming steady-state transport. This theoretical investigation consists of two steps. In the first step, we derive a model-based theoretical expression of the diffusion coefficient based on the continuity equation. Since this consideration is too simplified, in the second step, we perform Monte Carlo simulations to investigate how the electric field alters the electron occupation fraction of energy band valleys; for this, quantum mechanical scattering events during transport are calculated. Using these calculations, the electric field dependence of the diffusion coefficients of Ge and 4H-SiC wires with various cross-sectional areas is investigated because the conduction process of such materials is strongly ruled by the multi-valley transport of electrons. The obtained results reveal that the diffusion coefficient of Ge wires is constant when the electric field rises at 200 K and 400 K; but it rebounds under very high electric fields above 400 K due to the increase in the intrinsic carrier concentration. On the other hand, it is shown that the diffusion coefficient of 4H-SiC wires increases as the electric field rises in a low electric field range regardless of temperature, but it drops under high electric fields. Thus, it is considered that the theoretical models assumed for various semiconductor wires are useful in estimating the steady-state transport characteristics of scaled devices in a practical range of temperatures around room temperature.

***Keywords*—** Electric field; Diffusion coefficient; Semiconductor wires; Steady-state transport characteristics.

1. INTRODUCTION

The transport properties of one-dimensional materials, which include semiconductor wires of Si, Ge, and other materials, are attracting intense attention because such materials can realize energy-conversion devices through the Seebeck effect [1-4] and the photochemical effect [5]. Even though extensive simulation studies of such structures have been performed [6], several physical parameters must be reconsidered because various bulk properties of such materials are expected to alter with scale reduction [6]. The author's group has already investigated possible theoretical expressions of the diffusion coefficient of nanometer scale wires [7-9], and its viability has been examined numerically for Si [7, 8], Ge [9], and SiC nanowires [10]. Those studies demonstrated that the electron occupation fraction in each energy band determines the diffusion coefficient of nanowires, and that energy band valley non-parabolicity does not significantly influence the behavior of the diffusion coefficient because most electrons occupy a lower energy range at thermal equilibrium. In this paper, the carrier diffusion process in semiconductor materials like Si, Ge and SiC under an external

* Corresponding author
DOI: https://doi.org/10.5455/jjee.204-1711432905

electric field is revisited, and some theoretical models and numerical approaches are considered to predict the impact of external electric fields on the diffusion coefficient; one of the primary goals of this study is to reveal the validity of material analysis techniques because such considerations based on possible theoretical models have not yet been performed. Since band-to-band transitions should play an important role in determining the level of electron occupation in each energy band valley, carrier scattering processes are taken into account in formulating a theoretical expression of the diffusion coefficient; this analysis is performed by the Monte Carlo simulation technique. Though it is expected that the influence of the above difference on the diffusion coefficient is prominent in the nanometer range [10-13], this paper does not address this range of wire dimensions, as a preliminary study, because the practical formulation is too complex and its expected expression is not realistic in various applications. Thus, just the primary aspects of the influences of the electric field on the diffusion coefficient are extracted and discussed with the assumption of steady state transport.

2. THEORETICAL MODEL BASED ON PROBABILITY DENSITY AND IMPACTS OF EXTERNAL ELECTRIC FIELD

2.1. Theoretical Basis in the Thermal Equilibrium State

The author's group [11] proposed the basic mathematical model for the diffusion coefficient of nanoscale rectangular wires made from covalent semiconductors like Si, Ge, and SiC without any external electric field. Schematic energy band diagrams are shown in Fig. 1.

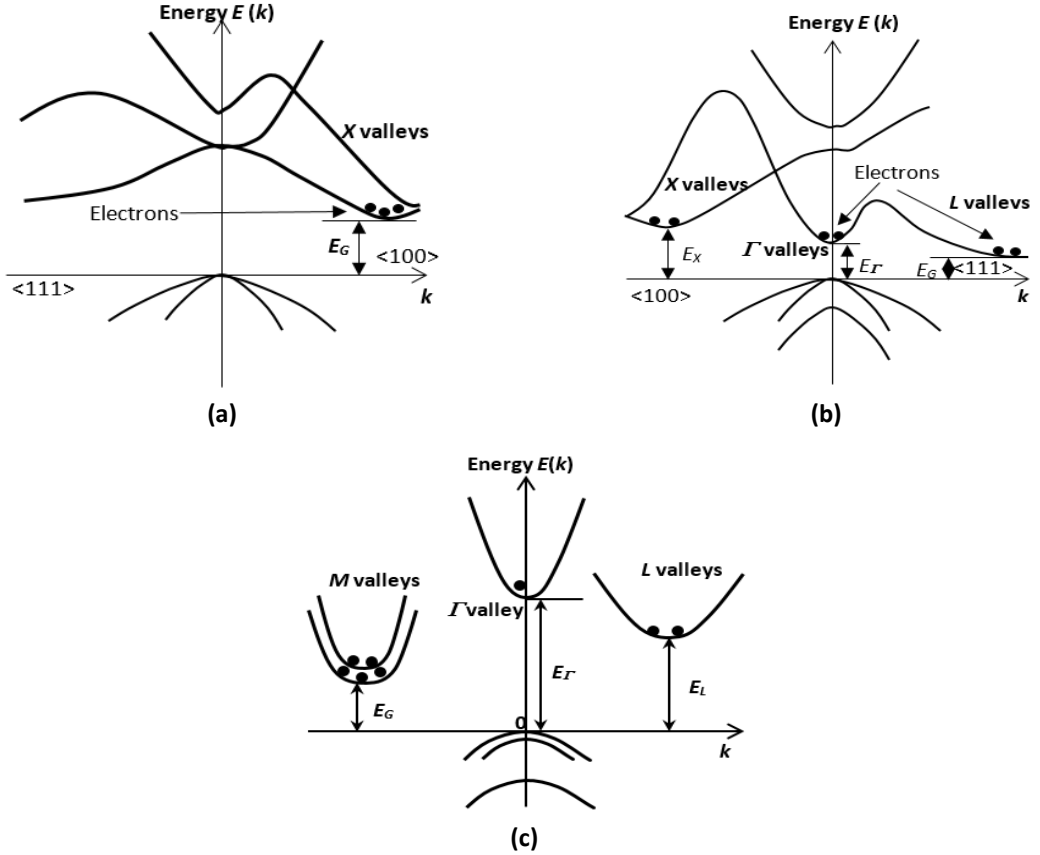

Fig. 1. Schematic energy band images of: a) Si; b) Ge; c) 4H-SiC [10].

The diffusion process is theoretically described by the master equation based on the probability density [14]. For the one-dimensional (1D) transport system of Si wires, for example,

we can assume single-valley transport. Therefore, the semi-classical diffusion coefficient $D_{Si}(\omega)$ is expressed as [11-20].

$$D_{Si}(\omega) = \sum_{x,x'} \left(-\frac{1}{2}\omega^2 \right) (x-x')^2 \tilde{P}_{Si}(x, i\omega \mid x') \tag{1}$$

where $\tilde{P}_{Si}(x, i\omega \mid x')$ is the Fourier transformation of the probability density of finding a particle at site x on the Si wire. This form was extended to cover real-world situations by using the approximate calculation technique. By making a couple of approximations, we derive the practical expression of $D_{Si,1D}$ as [11]:

$$D_{Si,1D} = \frac{1}{2}\tilde{T}_{Si} \left\langle v^2 \right\rangle_{Si} \tag{2}$$

where $\tilde{T}_{Si}$ is the characteristic time restricting the primary spectrum of carrier diffusion and $\left\langle v^2 \right\rangle_{Si}$ is the averaged value of squared velocity. A comparison with past simulation results [11] revealed that such mathematical calculations are sufficient for estimating material properties.

In contrast, for multiple-band transport, demonstrated by Ge, we have the following form without any external electric field [13].

$$\begin{aligned} D_{Ge}(\omega) = {} & p_X \sum_{x,x'} \left(-\frac{1}{2}\omega^2 \right) (x-x')^2 \tilde{P}_{Ge,X}(x, i\omega \mid x') + p_L \sum_{x,x'} \left(-\frac{1}{2}\omega^2 \right) (x-x')^2 \tilde{P}_{Ge,\mathrm{L}}(x, i\omega \mid x') \\ & + p_\Gamma \sum_{x,x'} \left(-\frac{1}{2}\omega^2 \right) (x-x')^2 \tilde{P}_{\mathrm{Ge},\Gamma}(x, i\omega \mid x') \end{aligned} \tag{3}$$

where p_X, p_L, and p_Γ are the occupation fractions of X valley, L valley, and Γ valley, respectively [13]. $\tilde{P}_{Ge,\mathrm{X}}(x, i\omega \mid x')$, $\tilde{P}_{Ge,\mathrm{L}}(x, i\omega \mid x')$, and $\tilde{P}_{\mathrm{Ge},\Gamma}(x, i\omega \mid x')$ are the diffusion process probability components for the X valley, L valley, and Γ valley, respectively. Applying similar approximations to Eq. (3), yields the practical form for $D_{Ge,1D}$ as [13]:

$$D_{Ge,1D} = p_X D_{Ge,\mathrm{X}} + p_L D_{Ge,\mathrm{L}} + p_\Gamma D_{Ge,\Gamma} \tag{4}$$

where $D_{Ge,\mathrm{X}}$, $D_{Ge,\mathrm{L}}$, and $D_{Ge,\Gamma}$ are the diffusion coefficients in the X valley, L valley and Γ valley, respectively. A similar expression for $D_{\mathrm{SiC},1D}$ is obtained for 4H-SiC nanowires as [14]:

$$D_{\mathrm{SiC},1D} = p_L D_{\mathrm{SiC,L}} + p_{M1} D_{\mathrm{SiC,M1}} + p_{M2} D_{\mathrm{SiC,M2}} + p_\Gamma D_{\mathrm{SiC},\Gamma} \tag{5}$$

where the terminology follows that of Eq. (4). Theoretical calculation results yielded by Eqs. (4) and (5) for Ge and SiC wires led to many interesting findings [13- 21].

At the second step, however, we must have a realistic perspective of material properties in future applications because nanoscale materials may be used in the presence of other than low-electric fields. In the next subsection, an advanced theoretical formulation is introduced to handle the impact of an external electric field, assuming steady state transport, on the diffusion coefficient of semiconductor materials.

2.2. Theoretical Formulation of the Impact of an External Electric Field <I>

Several theoretical studies on the diffusion coefficient in the non-equilibrium condition have been published recently [22-24] that use Langevin's approach to investigate the fluctuation and chemical diffusion process. In contrast, this paper proposes two methods to take account

of the impact of external electric fields on the diffusion coefficient. We start with the first method. Assuming the electric field is not extremely high, the influence of the electric field on the diffusion coefficient for Si wires, wherein single-valley transport is dominant, can be covered by semi-classical and semi-empirical methods.

In this model, the impact of the velocity saturation of electrons under a high electric field on the diffusion coefficient is considered theoretically based on the conventional, semi-classical continuity equation.

$$\frac{\partial}{\partial x} J_n(x) = \frac{\partial}{\partial t} n(x) = 0, \tag{6}$$

where $J_n(x)$ and $n(x)$ are the electron current density in the one-dimensional flow and the electron density, respectively. It is assumed that $J_n(x)$ is uniform on the y-z plane. $J_n(x)$ is expressed as

$$J_n(x) = qn(x)\mu_n(F)F + qD_n(F)\frac{\partial n(x)}{\partial x} \tag{7}$$

where F is the longitudinal local electric field in the material, q denotes the elementary charge, $\mu_n(F)$ is electron mobility, and $D_n(F)$ is the diffusion coefficient. Under the steady state condition, the current continuity requires

$$\frac{\partial}{\partial x} J_n(x) = \frac{\partial}{\partial t} n(x) = 0 \tag{8}$$

This results in the following equations.

$$\frac{\partial}{\partial x} J_n(x) = K_0 + K_1 = 0 \tag{9}$$

$$K_0 = q\mu_n(F)F\frac{\partial n(x)}{\partial x} + qD_n(F)\frac{\partial^2 n(x)}{\partial x^2} \tag{10}$$

$$K_1 = qn(x)F\frac{\partial \mu(F)}{\partial F}\frac{\partial F}{\partial x} + qn(x)\mu(x)\frac{\partial F}{\partial x} + q\frac{\partial D_n(F)}{\partial F}\frac{\partial F}{\partial x}\frac{\partial n(x)}{\partial x} \tag{11}$$

The relation $K_0 = 0$ gives the conventional Einstein relation that is valid with low electric fields. Here, we use D_{n0} to identify the diffusion coefficient given by $K_0 = 0$.

This suggests that the relation of $K_1 = 0$ gives, approximately, the semi-classical expression for the electric-field effect on the diffusion coefficient. Based on this idea, we use D_{nF} to refer to the diffusion coefficient in the following. Calculation details are given in Appendix A.

The final form of the diffusion coefficient is given as

$$\begin{aligned} D_{Si}(F) &= D_{Si,0} + D_{Si,F}(F) \\ &= D_{Si,0}\left[1 + \frac{F_0 - F}{(F_0 + F_C)(F + F_C)} + \log\left(\frac{F}{F_0}\right) - \log\left(\frac{F + F_C}{F_0 + F_C}\right)\right] \end{aligned} \tag{12}$$

$$D_{Si,0} = \frac{k_B T}{q}\mu_0 \equiv D_{Si,1D} \tag{13}$$

where $D_{si,0}$ is equivalent to Eq. (2). F_0 and F_C are the effective lowest electric field and the critical electric field, respectively, and are defined in Appendix A. Eq. (12) is valid for $F > F_0$.

2.3. Theoretical Formulation on the Impact of External Electric Field <II>

The previous subsection detailed the theoretical model that considers the semi-classical effect of the external electric field on the diffusion coefficient, where the velocity saturation effect is the primary considered by the theoretical formulation. However, it is easily anticipated that the impact of the dynamic transition of electrons between energy valleys during transport can't be considered in sufficient detail. This subsection discusses the second method, which applies to the multi-valley transport system. With reference to the author's previous papers [13, 21], the theoretical expressions for the occupation fraction like p_X, p_L, and p_Γ for Ge, were introduced assuming thermal equilibrium. However, it is not easy to derive analytical expressions under high electric fields [22-24]. Accordingly, this paper introduces the Monte Carlo simulation technique to determine the valley occupation fraction under high electric fields.

Since it is assumed here, for simplicity, that the cross-section dimensions of the wire are larger than 10 nm, the electronic states are not quantized given that extremely low temperatures are not assumed, so the approximations for a three-dimensional transport system are available. When the parabolic energy band structure is assumed for simplicity, the scattering rate W(k) of electrons in the specific band by impurity scattering, acoustic phonon scattering, and optical phonon scattering processes can be expressed as a function of the wave number (k) as [25-27]:

(i) Impurity scattering rate

$$W_{imp}\left(k\right)=\frac{2\pi N_I Z^2 q^4 D_{os}\left(E_k\right)}{\hbar\varepsilon_S^2}\frac{1}{k_D^2\left(4k^2+k_D^2\right)} \tag{14}$$

$$D_{os}\left(E_k\right)=\frac{\left(2m_{valley}^{*}\right)^{3/2}\sqrt{E_k}}{4\pi^2\hbar^3} \tag{15}$$

(ii) Acoustic phonon scattering rate

$$W_{ac\_ph}\left(k\right)=\frac{2\pi\Xi_d^2 k_B T D_{os}\left(E_k\right)}{\hbar c_L} \tag{16}$$

(iii) Non-polar optical phonon scattering rate

$$W_{\mathrm{np\_opt\_}ph}^{\mathrm{int}ra}\left(k\right)=\frac{\pi D_{opt}^2\left(n_o+\frac{1}{2}\mp\frac{1}{2}\right)D_{os}\left(E_k\pm\hbar\omega_{opt}\right)}{\rho\omega_{opt}} \tag{17}$$

for intra-band scattering, and

$$W_{\mathrm{np\_opt\_}ph}^{ij}\left(k\right)=\frac{\pi D_{opt\_\mathrm{ij}}^2 Z_j\left(n\left(\omega_{opt\_ij}\right)+\frac{1}{2}\mp\frac{1}{2}\right)D_{os}\left(E_k\pm\hbar\omega_{opt\_ij}-\Delta E_{ij}\right)}{\rho\omega_{opt\_ij}} \tag{18}$$

for inter-band scattering.

(iv) Polar optical phonon scattering rate (for 4H-SiC)

$$W_{\mathrm{p\_opt\_}ph}\left(k\right)=\frac{q^2\omega_{opt}k\left(n\left(\omega_{opt}\right)+\frac{1}{2}\mp\frac{1}{2}\right)}{8\pi\varepsilon_p E_k}\log\left(\frac{k_{\max}}{k_{\min}}\right) \tag{19}$$

$$k_{\min}=k\left|1-\sqrt{1\pm\frac{\hbar\omega_{opt}}{E_k}}\right| \tag{20}$$

$$k_{\max} = k\left(1+\sqrt{1\pm\frac{\hbar\omega_{opt}}{E_k}}\right) \tag{21}$$

$$\frac{1}{\varepsilon_p} = \frac{1}{\varepsilon_\infty} - \frac{1}{\varepsilon_S} \tag{22}$$

where N_I is the density of the ionized impurity, Z is the atomic number, ε_S is the semiconductor's static permittivity, k_D is the Debye wave number, m^*_{valley} is the effective mass of electrons in the specific valley, E_k is the electron energy in the specific valley, Ξ_d is the deformation potential, c_L is the velocity of sound, D_{opt} is the optical deformation potential on the specific valley for intra-band scattering, ω_{opt} is the optical angular frequency in the specific valley for intra-band scattering, n_0 is the optical phonon density in the specific valley, D_{opt_ij} is the optical deformation potential for inter-band scattering, ω_{opt_ij} is the optical angular frequency inter-band scattering, Z_j is the number of patterns of inter-band scattering, ΔE_{ij} is the energy difference between two different valleys, and ε_∞ is the semiconductor's optical permittivity.

Since it is expected that the occupation fractions of energy valleys are a function of the time spent under the external electric field and the strength of the field, various combinations of such parameters are considered so that the simulation results apply to many cases.

When the occupation fractions of valleys are labeled, for Ge, as $p_L(F)$, $p_X(F)$, and $p_\Gamma(F)$, the diffusion coefficient for Ge wires can be expressed as:

$$D_{Ge}(F) = \sum_{i=L,X,\Gamma} p_i(F) D_{\mathrm{Ge,i}}\left[1+\frac{F_{0,i}-F}{\left(F_{0,i}+F_{C,i}\right)\left(F+F_{C,i}\right)}+\log\left(\frac{F}{F_{0,i}}\right)-\log\left(\frac{F+F_{C,i}}{F_{0,i}+F_{C,i}}\right)\right] \tag{23}$$

where $D_{Ge,i}$ (i=L, X, and Γ) is the diffusion coefficient component in each valley appearing in Eq. (4). $p_i(F)$ (i=L, X, and Γ) is the valley occupation fraction as a function of the electric field as calculated by Monte Carlo simulations. $F_{0,j}$ and $F_{C,j}$ (i=L, X, and Γ) are the effective lowest electric field and the critical electric field in each valley, respectively. For the case of 4H-SiC wires, the expression of the diffusion coefficient is obtained in a similar way. In the following consideration, for simplicity, it is assumed that $D_{Ge,L} = D_{Ge,X} = D_{Ge,\Gamma}$, $F_{0,L} = F_{0,X} = F_{0,\Gamma}$, and $F_{CL} = F_{C,X} = F_{C,\Gamma}$.

3. SIMULATION RESULTS AND DISCUSSION

3.1. Electric Field Dependence of Diffusion Coefficient of Various Semiconductor Wires

Figure 2 shows the physical confinement and transport configurations of the semiconductor rectangular wires assumed in this paper; Fig. 2(a) show a Si rectangular wire physically confined with (001) and (010) surfaces where the transport is along the <100> direction. Fig. 2(b) shows a Ge rectangular wire physically confined with (001) and (010) surfaces where multi-valley conduction is assumed; transport is along the <100> direction. Fig. 2(c) corresponds to wurtzite rectangular 4H-SiC wire, where multi-valley conduction is assumed and it is also assumed that the wire is physically confined with (0001) and $\{1\bar{1}20\}/\{11\bar{2}0\}$ surfaces; electrons flow along the $<\bar{1}100>$ axis. Parameters assumed in calculations are summarized in Table 1.

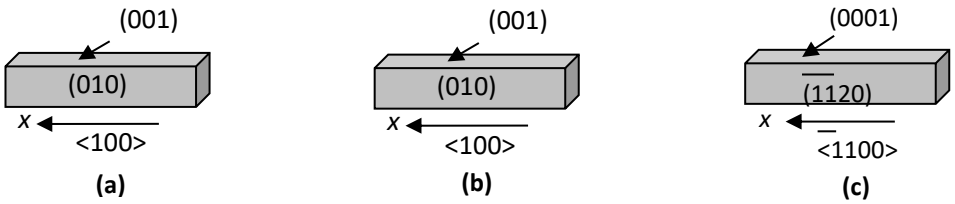

Fig. 2. Confinement and transport configuration assumed in this paper: a) Si wire; b) Ge wire; c) 4H-SiC wire with wurtzite structure.

Table 1. Physical parameters assumed in simulations.

Parameters [units]	Si	Ge	4H-SiC	Ref.
Energy bandgap*[eV]				
M1 valley	-	-	3.23	[28, 31, 32]
M2 valley	-	-	3.33	[28, 31, 32]
L valley	-	0.66	4.0	[28, 31, 33]
X valley	1.12	0.84	-	[28, 31, 34]
Γ valley	-	0.8	6.0	[28, 31-33]
Effective mass values of electrons**				
M1 valley				
m_{tM1}/m_0	-	-	0.42	[29, 30]
m_{lM1}/m_0	-	-	0.29	[29, 30]
M2 valley				
m_{tM2}/m_0	-	-	0.35	[29, 30]
m_{lM2}/m_0	-	-	0.71	[29, 30]
L valley				
m_{tL}/m_0	-	0.082	0.66	[29, 30, 35, 36]
m_{lL}/m_0	-	1.59	0.15	[29, 30, 35, 36]
X valley				
m_{tX}/m_0	0.19	0.29	-	[34, 37]
m_{lX}/m_0	0.98	1.35	-	[34, 37]
Γ valley				
m_Γ/m_0	-	0.04	-	[34]

*Measured from the valence band top (@300K).
**m_0 is the free space mass of electrons.

Figure 3 shows the calculation results of the electric field dependence of normalized diffusion coefficient ($D_{Si}(F)/D_{Si0}$) of Si wires at various temperatures. These calculations assumed that all the electrons occupy only 6 X valleys. Calculations assumed the steady state while the electric field is being applied to the wire. Fig. 3(a) shows the results for the doping level of $1x10^{15}$ cm^{-3} and Fig. 3(b) for the doping level of $1x10^{17}$ cm^{-3}. Some assumptions for temperature dependence of physical parameters are given in *Appendix B*. Figs. 3(a) and 3(b) reveal that the normalized diffusion coefficient ($D_{Si}(F)/D_{Si0}$) rises as the electric field is increased and as temperature rises. Such a behavior of the diffusion coefficient has been already discussed theoretically [35], where semi-classical particles in a liquid were assumed; it was shown that the diffusion coefficient is larger by 30% than that expected from conventional Brownian particles. It should be noted that $F_C \propto \exp(-T)$ and $F_0 \propto \sqrt{T}$ in Eq. (12), which suggests that the influence of the velocity saturation is weakened as temperature rises, but the influence of thermal potential becomes noticeable as temperature

rises. In other words, the diffusion potential due to thermal energy is enhanced in Fig. 3.

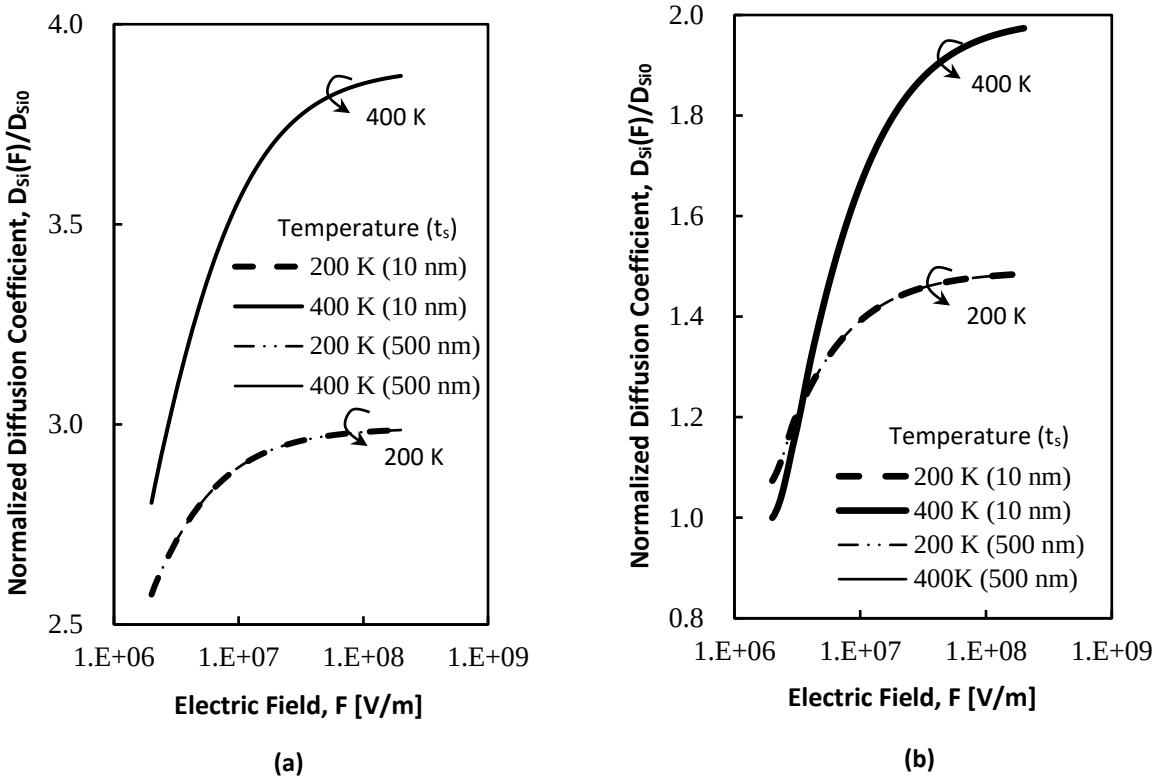

Fig. 3. Calculated $D_{Si}(F)/D_{Si0}$ values as a function of the external electric field (F) at various temperatures and for various cross-section dimensions of wires: a) $N_D=10^{15}$ cm^{-3}; b) $N_D=10^{17}$ cm^{-3}.

According to the study by Jacoboni's group [37], on the other hand, the increase in the diffusion coefficient of bulk Si can be discerned from Monte Carlo simulations, where a slight increase in the diffusion coefficient of electrons is expected but only in the medium electric field range. Then, since the difference between our result and Jacoboni's result suggests that the multi-valley transport must be taken into account, even in Si wires, the simplified model given here must investigated further in the future.

In Fig. 3, it is also seen that the simplified model is insensitive to the cross-sectional dimensions because the model does not include any term of dimension. On the other hand, it is sensitive to the doping level, and it is seen that increasing the doping level suppresses the temperature dependence of the normalized diffusion coefficient ($D_{Si}(F)/D_{Si0}$).

Figure 4 shows the calculation results of the electric field dependence of normalized diffusion coefficient ($D_{Ge}(F)/D_{Ge0}$) of Ge wires at various temperatures. In this calculation, it is assumed that the electrons occupy L valleys, X valleys, and Γ valley. Calculations assume the steady state while the electric field is being applied to the wire.

Fundamental aspects of Figs. 4(a) and 4(b) are the same as those of Figs. 3(a) and 3(b). Fig. 4 differs significantly from Fig. 3 in that the electric field dependence of $D_{Ge}(F)/D_{Ge0}$ is sensitive to the cross-section dimensions of the wire, and that the value of $D_{Ge}(F)/D_{Ge0}$ is decreased as temperature rises.

Since the occupation fraction of each energy valley is taken into account in calculating the diffusion coefficient, it is considered that the diffusion coefficient is sensitive to temperature due to the temperature dependence of the valley occupation fraction and the cross-section of the wire, although $D_{Ge}(F)/D_{Ge0}$ is not sensitive to the doping level. These behaviors are discussed in [13].

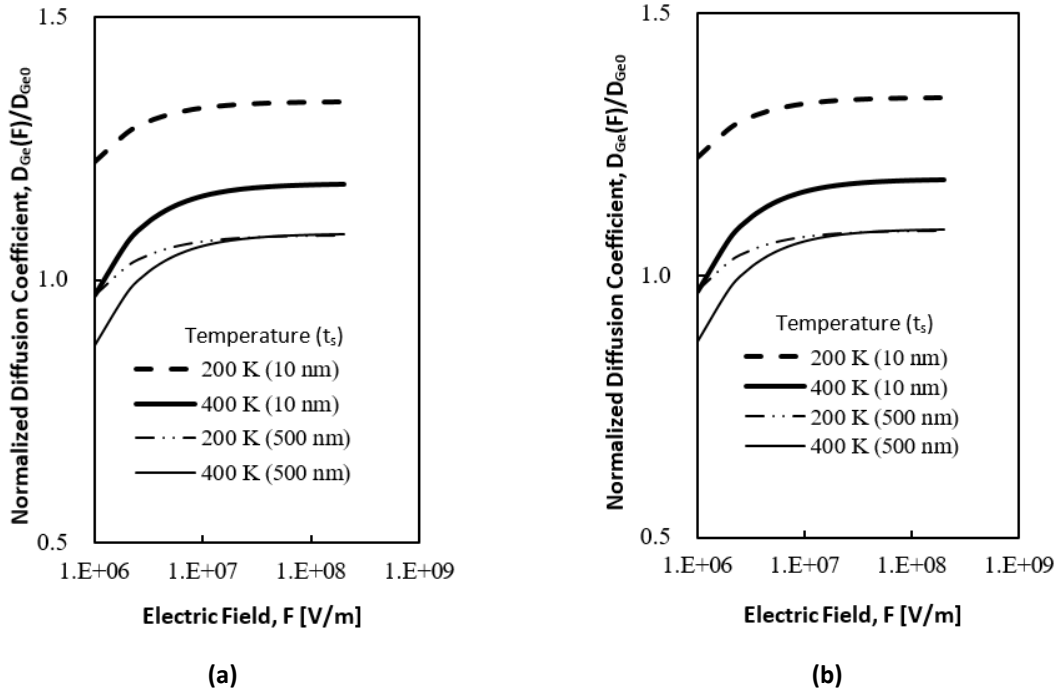

Fig. 4. Calculated $D_{Ge}(F)/D_{Ge0}$ values as a function of the external electric field at various temperatures and for various dimensions of cross-section of wires: a) N_D= 10^{15} cm^{-3}; b) N_D=10^{17} cm^{-3}.

Figure 5 shows the calculation results of the electric field dependence of normalized diffusion coefficient ($D_{SiC}(F)/D_{SiC0}$) of 4H-SiC wires at various temperatures. Calculations assumed the steady state while the electric field is being applied to the wire. Fundamental aspects of Figs. 5(a) and 5(b) are almost similar to those of Figs. 3 and 4. A significant difference between Figs. 4 and 5 is that the electric field dependence of $D_{Ge}(F)/D_{Ge0}$ is sensitive to the doping level, and that the temperature dependence of Fig. 5 is similar to that in Fig. 3, but different from that in Fig. 4. Since the occupation fraction of each energy valley is taken into account, it is considered that the diffusion coefficient is sensitive to temperature and the cross-section dimensions of the wire [21].

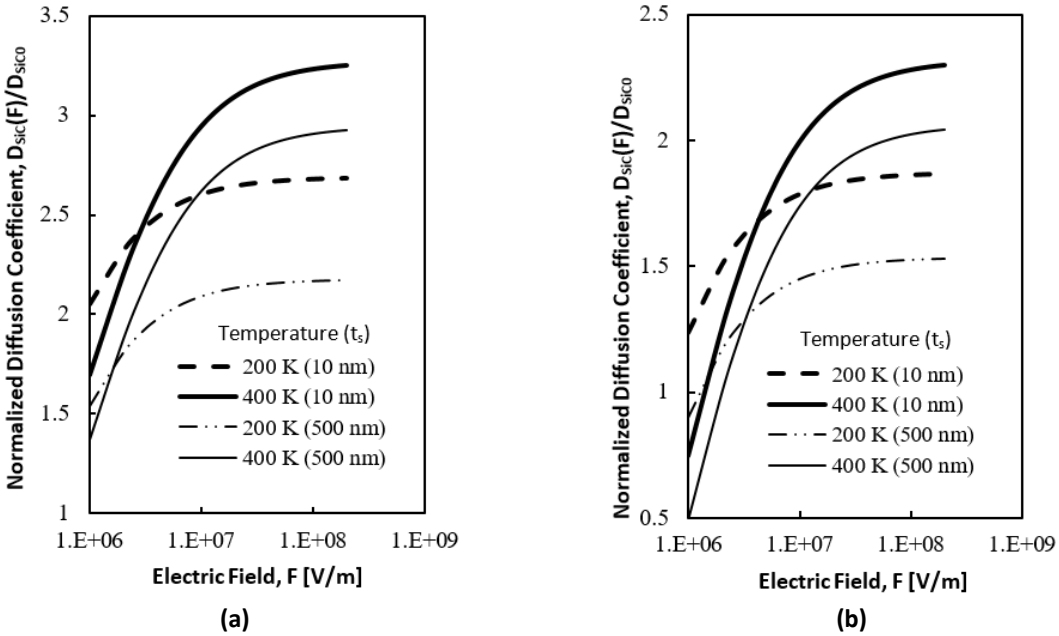

Fig. 5. Calculated $D_{SiC}(F)/D_{SiC0}$ values as a function of the external electric field at various temperatures and for various dimensions of wire cross-sections: a) N_D= 10^{15} cm^{-3}; b) N_D=10^{17} cm^{-3}.

This subsection has shown that the normalized diffusion coefficients of Si, Ge, and 4H-SiC wires increase as the electric field rises but then saturate. As shown in the paper by Jacoboni's group [38, 39], the diffusion coefficient of Si increases slightly as the electric field rises but then it decreases as the electric field rises, which is different from the behaviors shown in Figs. 3 to 5. It is anticipated that the multi-valley transport under the electric field should be directly taken into account for these semiconductor wires [13, 21, 39] because the scattering events yielded by high electric fields accelerate the band-to-band transition. However, the material parameters of Si needed in Monte Carlo simulations are not disclosed. So, this paper discusses this issue only for Ge and 4H-SiC wires with the aid of Monte Carlo simulations in the next subsection.

3.2. Impacts of Multi-Valley Transport on the Normalized Diffusion Coefficient

Here, this paper introduces various simulation results on the electric field effect on the energy valley occupation fractions and its impact on the diffusion coefficient values of materials like Ge and 4H-SiC wires. Material parameters assumed in the Monte Carlo simulations are summarized in Tables 1 and 2. It was assumed that all the electrons initially occupied the *L* valleys for Ge wires and *M* valleys for 4H-SiC wires.

Table 2. Material parameters in Monte Carlo simulations

Parameters [units]	Si	Ge	4H-SiC	Ref.
N_I (N_D) [/cm^3]	-	1x10^{15}, 1x10^{17}	1x10^{15}, 1x10^{17}	-
ε_S / ε_0	-	16.0	9.7	[32, 37, 39]
X_d /q [eV]	-	5.0~11.0	19.0	[32, 37, 39]
c_L [cm/s]	-	3.81	13.7	[32, 37, 39]
ρ [g/cm^3]	-	5.32	3.21	[32, 37, 39]
ω_{opt} [meV]	-	35.4	104	[32, 37, 39]
ω_{opt_ij} [meV]	-	27.6	85.4	[32, 37, 39]
D_{opt} /q [eV]	-	0.8x10^{10}~3.0x10^{10}	3.0x10^{10}~9.0x10^{10}	[32, 37, 39]
ε_∞ / ε_0	-	10.9	8.5	[32, 37, 39]
D_{opt_ij} /q [eV]	-	2.0x10^{10}~1.0x10^{11}	2.0x10^{10}~1.0x10^{11}	[32, 37, 39]
Z_j	-	4 and 6	3 and 3	[32, 37, 39]

In the Monte Carlo simulations, the influence of discrete energy levels in each energy valley on the carrier concentration and the diffusion coefficient is taken into account for the cross-section dimensions of 10 nm x 10 nm. Simulation results of valley occupation fractions as a function of electric field for Ge wires are shown for the doping level of 10^{15} cm^{-3} in Fig. 6, where simulation results at two different temperatures are shown. Simulations assumed steady state transport while the electric field was being applied to the wire; here the time spent under the electric field was assumed to be ~2 ps. It is seen that the *L*-valley occupation fraction linearly decreases for F > 1x10^6 V/m at 200 K, while it linearly decreases for F > 5x10^6 V/m at 400 K, but steeply rebounds for F > 6x10^8 V/m. It is considered that the steep increase in *L*-valley occupation fraction stems from the thermalization of carrier distribution in each valley and the increase in the intrinsic carrier concentration. In Fig. 6(b), the critical electric field under which the steep decrease begins is higher than that in Fig. 6(a). This is due to the large increase at 400 K in the electron concentration in the *L* valleys.

Monte Carlo simulation results of valley occupation fractions as a function of electric field for Ge wires are shown for the doping level of 10^{17} cm^{-3} in Fig. 7, where simulation results

at two different temperatures are shown. Fundamental aspects of Fig. 7 are basically the same as those in Fig. 6. It is seen that the valley occupation fraction is not sensitive to the doping level.

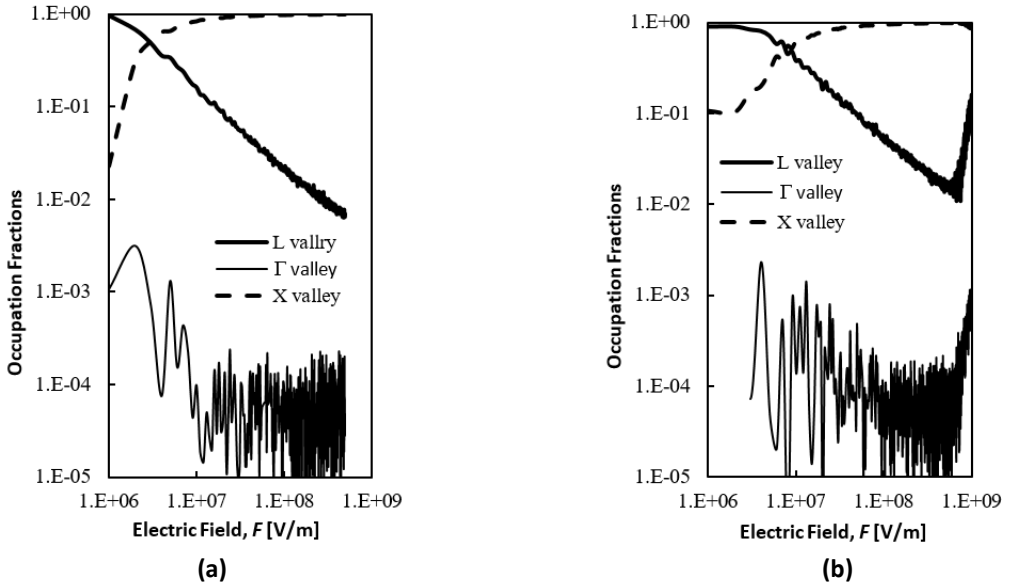

Fig. 6. Calculated valley occupation fraction of Ge wires as a function of the external electric field at various temperatures (t_s= 10 nm, N_D=10^{15} cm^{-3}): a) 200 K; b) 400 K.

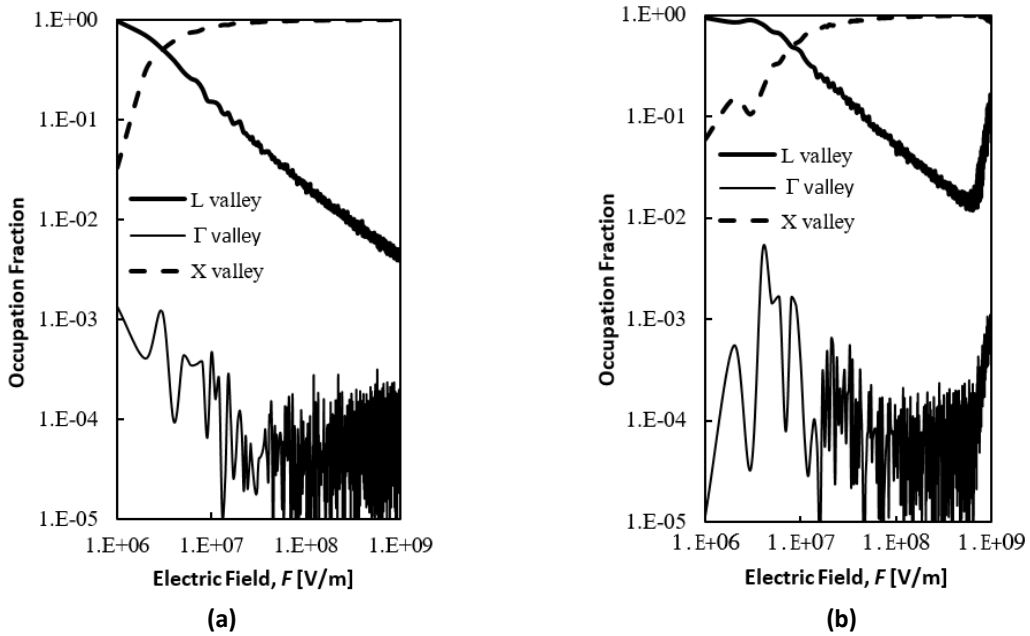

Fig. 7. Calculated valley occupation fraction of Ge wires as a function of the external electric field at various temperatures (t_s= 10 nm, N_D=10^{17} cm^{-3}): a) 200 K; b) 400 K.

In a similar way, Monte Carlo simulation results of valley occupation fractions as a function of electric field for 4H-SiC wires are shown for the doping level of 10^{15} cm^{-3} in Fig. 8, where simulation results at two different temperatures are shown. Simulations assumed steady state transport while the electric field was being applied to the wire; here the time spent under the electric field was assumed to be ~2 ps. It is seen that the *M*-valley occupation fraction drastically decreases for F > 1x10^7 V/m at 200 K, while, in contrast, the *L*-valley occupation fraction steeply increases for F > 10^7 V/m. In contrast to the case of Ge shown in Fig. 6, the behaviors of valley occupation fractions are not sensitive to temperature for 4H-SiC. It is anticipated that

4H-SiC has larger inter-valley gap than t Ge, and that in 4H-SiC has lower active electron concentration in the valley than Ge. Since the influence of the doping level is not significant, the simulation results for the doping level of $1x10^{17}$ cm^{-3} are not shown here.

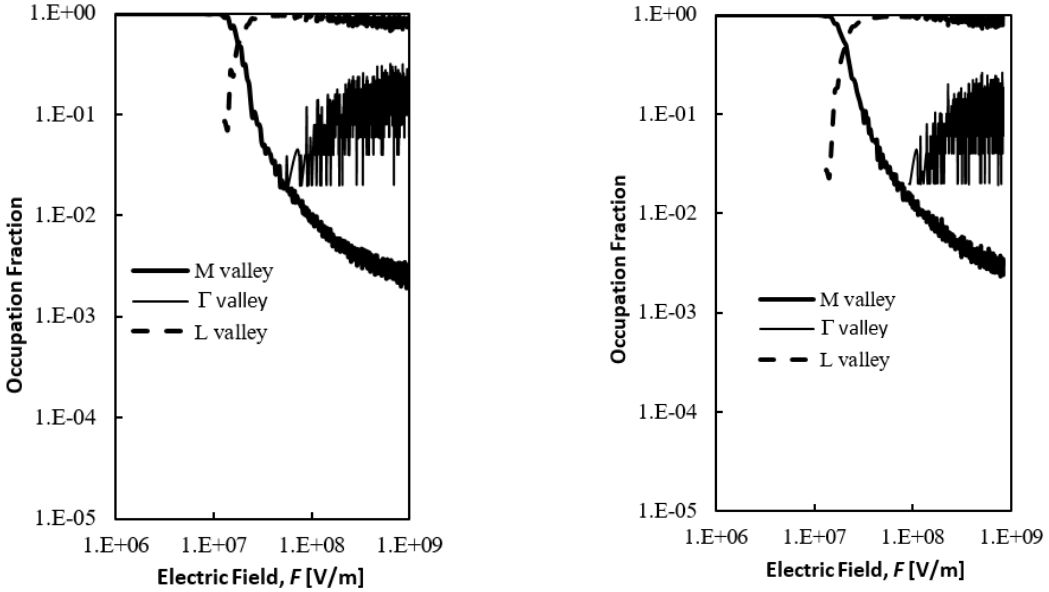

Fig. 8. Calculated valley occupation fraction of 4H-SiC wires as a function of the external electric field at various temperatures. (t_s= 10 nm, N_D=10^{15} cm^{-3}): a) 200 K; b) 400 K.

3.3. Electric Field Dependence of the Diffusion Coefficient

This subsection describes how the simulation results shown in Figs. 6 and 8 can be used in order to evaluate the impact of the electric field on the valley occupation fractions. Here, two-step calculations of the normalized diffusion coefficient are performed. In the first step, a set of piecewise equations that can reproduce Monte Carlo simulation results is created. In the second step, a combination of the set of piecewise equations and the diffusion coefficient calculation results yield the final result of the electric field dependency of the diffusion coefficient.

Figure 9 shows the calculation results of the normalized diffusion coefficient of Ge wires with three different cross-sectional dimensions at 200 K and 400 K. Fig. 9(a) reveals that the diffusion coefficient is slightly increased in a low electric field range at 200 K and clearly decreased in a high electric field range. Fig. 9(b), in contrast, reveals that at 400 K it falls in a medium electric field range and steeply rebounds in a high electric field range. In both cases, the normalized diffusion coefficient is not so sensitive to the wire's cross-section dimensions. Aspects of behaviors of the normalized diffusion coefficients are roughly identical to those seen in Fig. 6.

Figure 10 shows the calculation results of the normalized diffusion coefficient of 4H-SiC wires with three different cross-sectional dimensions at 200 K and 400 K. Fig. 10(a) reveals that at 200 K the diffusion coefficient increases as the electric field rises to $1x10^7$ V/m but decreases in a high electric field range. A similar behavior of the normalized diffusion coefficient is also seen in Fig. 10 (b). In both cases, the normalized diffusion coefficient is slightly sensitive to wire cross-section dimensions. Aspects of behaviors of the normalized diffusion coefficients roughly track those seen in Fig. 8.

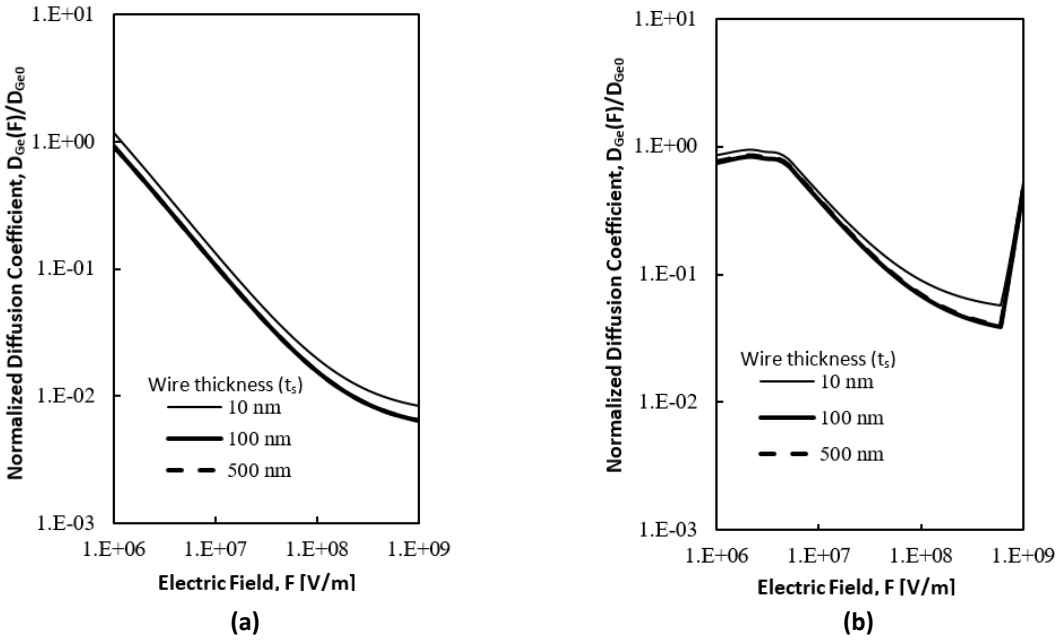

Fig. 9. Calculated normalized diffusion coefficient of Ge wires as a function of the external electric field for various thicknesses (N_D=10^{15} cm^{-3}): a) 200 K; b) 400 K.

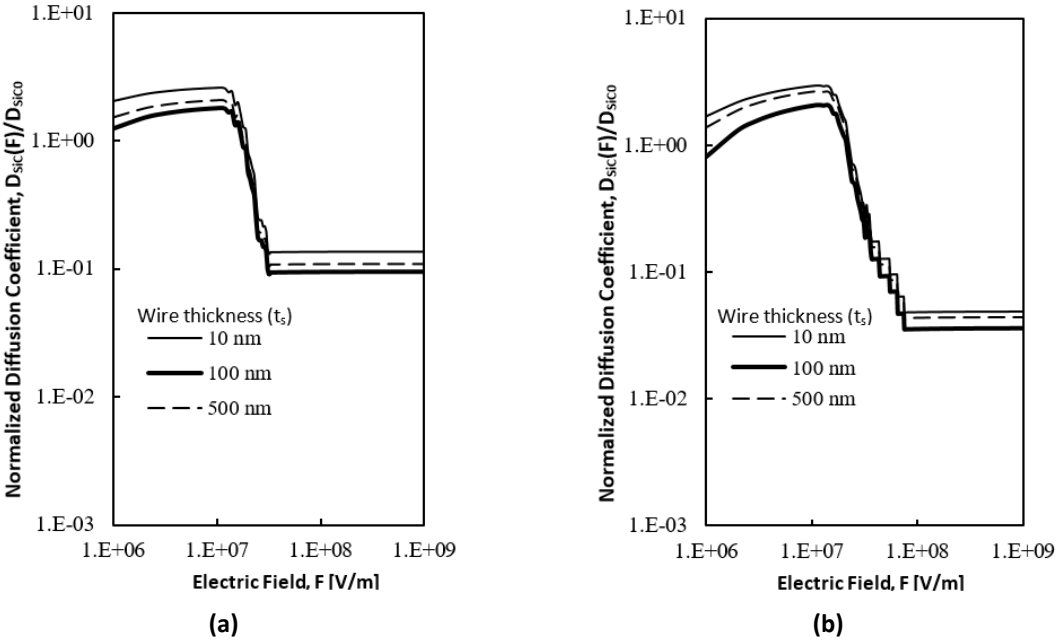

Fig. 10. Calculated normalized diffusion coefficient of 4H-SiC wires as a function of the external electric field for various cross-section dimensions (N_D=10^{15} cm^{-3}):: a) 200 K; b) 400 K.

3.4. Future Issues

The theoretical discussion of this paper is limited to the wire materials shown in Fig. 2 because our purpose is to examine the method and the model. However, it has already been demonstrated for Si and Ge wires that the diffusion coefficient depends on physical confinement [12, 13]. Therefore, it is anticipated that the diffusion coefficients of Ge and SiC wires are also sensitive to physical confinement. While many reliable physical parameters of Ge and SiC materials have been revealed by energy band analysis and related experiments, even more reliable predictions of the diffusion coefficient of Ge and SiC materials will become possible. SiC materials are seen as promising for high-voltage applications due to their large

bandgap [40]. Moreover, such large bandgap materials are necessary in space electronics because device degradation due to high-energy radiation must be suppressed [41]. In addition, wire-type gate-all-around (GAA) MOS devices [42] are very promising for space applications because their small device volume results in less degradation by high-energy radiation. For future device design [43], physical parameters like the diffusion coefficient play an important role in enhancing design reliability. Therefore, analyses of material parameters remain essential in predicting optimum device architectures.

3.5. CONCLUSIONS

This paper investigated how the diffusion coefficients of various semiconductor wires are influenced by an external electric field assuming steady state transport. This issue was investigated in two steps. In the first step, this paper derived a model-based theoretical expression of the diffusion coefficient based on the continuity equation, where the velocity saturation effect is taken into account and single-valley transport is assumed for simplicity. The theoretical expression revealed that the electric field increases the diffusion coefficient of wires regardless of temperature and wire cross-sectional area. However, this does not match past Monte Carlo simulation results for Si bulk material. So, in the second step, this paper performed Monte Carlo simulations in order to investigate how the electric field modifies the electron occupation fraction of energy band valleys during transport, where quantum mechanical scattering events were taken into account. As multi-valley transport plays an important role in Ge and 4H-SiC wires, this method was used in calculating valley-occupation fraction values. Using these calculations, electric field dependence of the diffusion coefficients of Ge and 4H-SiC wires having various cross-sectional areas was investigated.

It was shown that the behaviors of the diffusion coefficient of Ge wires are sensitive to temperature, but not to wire cross-sectional area. It was also shown that the diffusion coefficient of Ge wires basically remains unaltered as the electric field rises at 200 K and 400 K, but that it rebounds in a very high electric field at 400 K due to the increase in the intrinsic carrier concentration. On the other hand, it is seen for 4H-SiC wires that the diffusion coefficient is definitely increased as the electric field rises in a low electric field range regardless of temperature, but it steps down in a high electric field range. It was also seen that the diffusion coefficient of 4H-SiC wires is sensitive to the wire cross-sectional area.

Thus, it is considered that the conventional theoretical models assumed for various semiconductor wires are basically useful in estimating the transport characteristics of scaled devices at various temperatures around room temperature. When more physical parameters of other semiconductor materials are determined accurately, more reliable predictions of the diffusion coefficient of such materials and other materials for future applications like energy conversion will become possible.

APPENDIX A: SEMI-CLASSICAL MODEL OF THE ELECTRIC FIELD INFLUENCE ON THE DIFFUSION COEFFICIENTS

As noted in Section 2, the solution of $K_1 = 0$ is calculated here. From Eq. (11), we have

$$\frac{\partial D_{nF}(F)}{\partial F} = \frac{-n(x)}{\left(\frac{\partial n(x)}{\partial x}\right)}\left[F\frac{\partial \mu(F)}{\partial F} + \mu(x)\right] \quad \text{(A. 1)}$$

When it is assumed that electron density n(x) has the form of a shifted Boltzmann distribution [44], we can assume the electron density has the following form with local potential ϕ.

$$n(\phi) = n_0 \exp\left(\frac{q\phi}{k_B T}\right) \tag{A. 2}$$

In addition, we have

$$\begin{aligned}\frac{\partial n(\phi)}{\partial} &= n(\phi)\left(\frac{q}{k_B T}\right)\left(\frac{\partial \phi}{\partial x}\right) \\ &= -n(\phi)\left(\frac{q}{k_B T}\right)F\end{aligned} \tag{A. 3}$$

Combining Eq. (A.1) with Eq. (A.3) leads us to

$$\frac{\partial D_{nF}(F)}{\partial F} = \left(\frac{k_B T}{q}\right)\left[\frac{\partial \mu(F)}{\partial F} + \frac{\mu(x)}{F}\right] \tag{A. 4}$$

In order to integrate Eq. (A.4), a simple mobility model is introduced as a preliminary consideration [45].

$$\mu_n(F) = \frac{\mu_0}{1 + F / F_c} \tag{A. 5}$$

$$F_C = \frac{v_{Sat}}{\mu_0} \tag{A. 6}$$

where μ_0 is the low-field mobility, F_c is the critical electric field causing the velocity saturation, and v_{Sat} is the saturation velocity.

Integration of Eq. (A.4) gives us the following solution of $D_{nF}(F)$ for $F>F_0$.

$$\begin{aligned}D_{nF}(F) &= \left(\frac{k_B T}{q}\right)\int_{F_0}^{F}\left[\frac{\partial \mu(F')}{\partial F'} + \frac{\mu(x)}{F'}\right]dF' \\ &= \left(\frac{k_B T}{q}\mu_0\right)\left[\frac{F_0 - F}{(F_0 + F_C)(F + F_C)} + \log\left(\frac{F}{F_0}\right) - \log\left(\frac{F + F_C}{F_0 + F_C}\right)\right]\end{aligned} \tag{A. 7}$$

where F_0 means the lowest effective electric field in the material, which this paper assumes has the following definition.

$$F_0 = \left(\frac{k_B T}{q}\right) / L_D \tag{A. 8}$$

where L_D is the Debye length. Eq. (A.8) shows that F_0 stands for the effective local electric field originating from the electron density fluctuation in the material without any external electric field.

Then, the final form of diffusion coefficient $D_n(F)$ for $F>F_0$ can be expressed as

$$\begin{aligned}D_n(F) &= D_0 + D_{nF}(F) \\ &= D_0\left[1 + \frac{F_0 - F}{(F_0 + F_C)(F + F_C)} + \log\left(\frac{F}{F_0}\right) - \log\left(\frac{F + F_C}{F_0 + F_C}\right)\right]\end{aligned} \tag{A. 9}$$

$$D_0 = \frac{k_B T}{q}\mu_0 \tag{A. 10}$$

APPENDIX B: SUMMARY OF TEMPERATURE DEPENDENCE OF PHYSICAL PARAMETERS

In this paper, it is assumed that the transport in Si wires is by single-valley conduction. Electron concentration and hole concentration are expressed as, respectively

$$n_{n0}(0,T)=\frac{N_D}{1+\frac{1}{2}\exp\left(\frac{E_D-E_F(0)}{k_BT}\right)} \tag{B.1}$$

$$p_{p0}(0,T)=\frac{N_A}{1+4\exp\left(\frac{E_A-E_F(0)}{k_BT}\right)} \tag{B.2}$$

Then, the Fermi level of Si wires is given by [13]

$$E_D-E_F(0)=2\ln(2)\cdot k_BT -k_BT\ln\left[\sqrt{1+8\frac{N_D}{N_C}\exp\left(\frac{E_C-E_D}{k_BT}\right)}-1\right] \tag{B.3}$$

$$E_A-E_F(0)=-\ln(8)\cdot k_BT +k_BT\ln\left[\sqrt{1+16\frac{N_A}{N_V}\exp\left(\frac{E_A-E_V}{k_BT}\right)}-1\right] \tag{B. 4}$$

where N_D, N_A, E_D, E_A, E_F, N_C, and N_V take the conventional meanings. For degenerate p-type Si films, Eqs. (B. 2) and (B. 4) are applied in the simulations.

The Fermi level of n-type 4H-SiC wires is given by [13]:

$$E_F=E_D-(\ln 4)k_BT+k_BT\ln\left[-1+\sqrt{1+8\left(\frac{N_Dt_S^2}{I_L+I_M+I_\Gamma}\right)}\right] \tag{B. 5}$$

$$I_L=\frac{3}{\pi\hbar}\sqrt{2\pi m^*_{de,L}k_BT}\exp\left(-\frac{E_{\mathrm{L},00}-E_D}{k_BT}\right) \tag{B. 6}$$

$$I_{M1}=\frac{3}{\pi\hbar}\sqrt{2\pi m^*_{de,\mathrm{M1}}k_BT}\exp\left(-\frac{E_{\mathrm{M1},00}-E_D}{k_BT}\right) \tag{B. 7}$$

$$I_{M2}=\frac{3}{\pi\hbar}\sqrt{2\pi m^*_{de,\mathrm{M2}}k_BT}\exp\left(-\frac{E_{\mathrm{M2},00}-E_D}{k_BT}\right) \tag{B. 8}$$

$$I_\Gamma=\frac{1}{\pi\hbar}\sqrt{2\pi m^*_{de,\Gamma}k_BT}\exp\left(-\frac{E_{\Gamma,00}-E_D}{k_BT}\right) \tag{B. 9}$$

The Fermi level of Ge wires is also given in a way similar to Eqs. (B.5) to (B.9) [13]. Band-gap energy of Si, Ge, and 4H-SiC wires is expressed as [40, 42]

$$E_G(T) = E_{G0}(0) - \frac{\alpha T^2}{T+\beta} \quad \text{(B. 10)}$$

Saturation velocity of Si, Ge, and 4H-SiC wires is expressed as

$$v_{sat} = \frac{2.47\times10^5}{1.0+0.8\exp(T/600.0)} \text{ [m/s] for electrons in Si [40],} \quad \text{(B. 11)}$$

$$v_{sat} = \frac{2.75\times10^5}{1.0+\exp(T/300.0)} \text{ [m/s] for electrons in Ge [41],} \quad \text{(B. 12)}$$

$$v_{sat} = \frac{2.0\times10^5}{0.85+0.15(T/300.0)} \text{ [m/s] for electrons in SiC [37]} \quad \text{(B. 13)}$$

Low field mobility of electrons is expressed as

$$\mu_0 = 4.5\times10^{-2}\left(\frac{T}{300.0}\right)^{-2.2} \text{ [m}^2\text{/Vs] for electrons in Si [42]} \quad \text{(B. 14)}$$

$$\mu_0 = 3.9\times10^{-2}\left(\frac{T}{300.0}\right)^{-1.66} \text{ [m}^2\text{/Vs] for electrons in Ge [41]} \quad \text{(B. 15)}$$

$$\mu_0 = 9.5\times10^{-2}\left(\frac{T}{300.0}\right)^{-2.25} \text{ [m}^2\text{/Vs] for electrons in SiC [36]} \quad \text{(B. 16)}$$

REFERENCES

[1] L. Hicks, M. Dresselhaus, "Effect of quantum-well structures on the thermoelectric figure of merit," *Physical Review B*, vol. 47, pp. 12727-12731, 1993, doi: 10.1103/PhysRevB.47.1272.

[2] A. Hochbaum, R. Chen, R. Delgado, W. Liang, E. Garnett, M. Najarian, A. Majumdar, P. Yang, "Enhanced thermoelectric performance of rough silicon nanowires," *Nature*, vol. 451, pp. 163-167, 2008, doi: 10.1038/nature06381.

[3] L. Hicks, M. Dresselhaus, "Thermoelectric figure of merit of a one-dimensional conductor," *Physical Review B*, vol. 47, pp. 16631, 1993; doi: 10.1103/physrevb.47.16631.

[4] A. Boukai, Y. Bunimovich, J. Kheli, J. Yu, W. Goddard III, J. Heath, "Silicon nanowires as efficient thermoelectric materials," *Nature*, vol. 451, pp. 168-171, 2008, doi: 10.1038/nature06458.

[5] C. Xiang, A. C. Meng, N. Lewis, "Evaluation and optimization of mass transport of redox species in silicon microwire-array photoelectrodes," *Chemistry*, vol. 109, no. 39, pp. 15622-15627, 2012, doi: 10.1073/pnas.1118338109.

[6] P. Martin, Z. Aksamija, E. Pop, U. Ravaioli, "Impact of phonon-surface roughness scattering on thermal conductivity of thin Si nanowires," *Physical Review Letters*, vol. 102, p. 125503, 2009, doi: 10.1103/PhysRevLett.102.125503.

[7] S. Sato, Y. Omura, "Possible theoretical models for carrier diffusion coefficient of one-dimensional Si wire devices," *Japanese Journal of Applied Physics*, vol. 54, no. 5, p. 054001, 2015, doi: 10.7567/JJAP.54.054001.

[8] Y. Omura, S. Sato, '' Nanotechnology 1,'' *Universal Nanotechnology Skills Creation and Motivation Development*, 2017, http://www.onecentralpress.com/wp-content/uploads/2017/06/functional-nanostructures-proceedings-paper-01.pdf**.**

[9] Y. Omura, "Theoretical assessment of impacts of crystal orientation and energy band valley occupation on diffusion constant of nano-scale rectangular Ge wires," *ECS Journal of Solid-State Science and Technology*, vol. 11, no. 3, pp. 033005-1-0033005-13, 2022, doi: 10.1149/2162-8777/ac557a.

[10] M. Tutt, C. McAndrew, "Physical and numerically stable linvill-lump compact model of the pn-junction," *IEEE Journal of the Electron Devices Society*, vol. 4, no. 2, pp. 90-98, 2016, doi: 10.1109/JEDS.2016.2517190.

[11] K. Kim, T. Tang, S. Kim, "Accuracy balancing for the simulation of gate-all-around junctionless nanowire transistors using discrete Wigner transport equation," *AIP Advances*, vol. 8, p. 115105, 2018, doi: 10.1063/1.5055686.

[12] Y. Yang, H. Yang, G. Wei, L. Wang, M. Shang, Z. Yang, B. Tang, W. Yang, "Enhanced field emission of p-type 3C-SiC nanowires with B dopants and sharp corners", *Journal of Materials Chemistry C*, vol. 2, pp. 4515-4520, 2014, doi: 10.1039/C4TC00524D.

[13] C. Chen, S. Chen, M. Shang, F. Gao, Z. Yang, Q. Liu, Z. He, W. Yang, "Fabrication of highly oriented 4H-SiC gourd-shaped nanowire arrays and their field emission properties," *The Royal Society of Chemistry, Journal of Material Chemistry C*, vol. 4, pp.5195-5201, 2016, doi: 10.1039/C6TC00450D.

[14] X. Shiyu, "High quality 4H-SiC crystal growth and dislocations behavior during solution method," Ph. D. Thesis, Nagoya University, 2016.

[15] S. Mao, J. Liu, Y. Wang, W. Liu, J. Yao, Y. Hu, H. Cui, Z. Kong, R. Zhang, H. Liu, Z. Wang, T. Li, N. Zhou, Y. Zhang, J. Gao, Z. Wu, Y. Li, J. Li, J. Luo, W. Wang, H. Yin, "Ultralow contact resistivity on Ga-doped Ge with contact Co-implantation of Ge and B," *ECS Journal of Solid State Science and Technology*, vol. 11, p. 054002, 2022, doi: 10.1149/2162-8777/ac697a.

[16] T. Odagaki, M. Lax, "Coherent-medium approximation in the stochastic transport theory of random media," *Physical Review B*, vol. 24, p. 5284, 1981, doi: 10.1103/PhysRevB.24.5284.

[17] Y. Omura, "Theoretical prediction on temperature dependence of diffusion coefficient of various SiC nanowires," Workshop on Low-Temperature Electronics, doi: 10.1109/WOLTE55422.2022.9882545.

[18] X. Wang, W. Deng , Y. Chen, "Ergodic properties of heterogeneous diffusion processes in a potential well," *Journal of Chemical Physics*, vol. 150, p. 164121, 2019, doi: 10.1063/1.5090594.

[19] H. Han, S. Joo, T. Sakaue, J. Jeon, "Nonequilibrium diffusion of active particles bound to a semiflexible polymer network: Simulations and fractional Langevin equation," *Journal of Chemical Physics*, vol. 159, p. 024901, 2023, doi: 10.1063/5.0150224.

[20] P. Pravatto, B. Fresch, G. J. Moro," Large barrier behavior of the rate constant from the diffusion equation," *Journal of Chemical Physic*s, vol. 158, p. 144110, 2023, doi: 10.1063/5.0143522.

[21] K. Tomizawa, *Simulation of Submicron Semiconductor Devices*, 1993, Artech House Publishers.

[22] K. Hess, *Advanced Theory of Semiconductor Devices*, 2000, Wiley-IEEE Press.

[23] M. Lundstrom, *Fundamentals of Carrier Transport*, 2000, Cambridge University Press.

[24] G. Pennington, N. Goldsman, "Self-consistent calculations for n-type hexagonal SiC inversion layers," *Journal of Applied Physics*, vol. 95, pp. 4223-4234, 2004, doi: 10.1063/1.1687977.

[25] N. Ashraf, D. Vasileska, ''D. Ferry, Consistent Parameter Set for an Ensemble Monte Carlo Simulator Used for Describing Experimental Low-Field and High-Field Transport Parameters of 4H-SiC'', 2008, https://www.researchgate.net/publication/268368471.

[26] F. Leonardis, R. Soref, V. Passaro, "Dispersion of nonresonant third order nonlinearities in Silicon Carbide," *Scientific Report*, vol. 7, pp. 40924-1-40924-12, 2017; doi: 10.1038/srep40924.

[27] J. Wozny, A. Kovalchuk, Z. Lisik, J. Podgorski, P. Bugalski, A. Kubiak, L. Ruta, "Monte Carlo simulations of electron transport in 4H-SiC using the DFT-calculated density of states," *Journal of Computational Electronics*, vol. 20, pp. 791-797, 2021, doi: 10.1007/s10825-021-01658-y.

[28] *SiC- Silicon Carbide*, 2001, http://www.ioffe.ru/SVA/NSM/Semicond/SiC/basic.html.

[29] S. Sze, K. Ng, *Physics of Semiconductor Devices*, 2007, John Wiley & Sons.

[30] Y. Lee, M. McLennan, G. Klimeck, R. Lake, S. Datta, "Quantum kinetic analysis of mesoscopic systems: Linear response," *Superlattices and Microstructures*, vol. 11, pp. 137-140, 1992, doi: 10.1016/0749-6036(92)90237-Y.

[31] Y. Niquet, C. Delerue, "Carrier mobility in strained Ge nanowires," *Journal of Applied Physics*, vol. 112, p. 084301, 2012, doi: 10.1063/1.4759346.

[32] C. Jacoboni, L. Leggiani, "The Monte Carlo method for the solution of charge transport in semiconductors with applications to covalent materials," *Review of Modern Physics*, vol. 55, pp. 645-655, 1983, doi: 10.1103/RevModPhys.55.645.

[33] A. Ryabov, M. Tasinkevych, "Diffusion coefficient and power spectrum of active particles with a microscopically reversible mechanism of self-propelling," *Journal of Chemical Physics*, vol. 157, p. 104108, 2022, doi: 10.1063/5.0101520.

[34] C. Jacoboni, F. Nava, C. Canali, G. Ottaviani, "Electron drift velocity and diffusivity in germanium," *Physical Review B,* vol. 24, pp. 1014-1026, 1981, doi: 10.1103/PhysRevB.24.1014.

[35] G. Rajendran, C. Vaithilingam, K. Naidu, K. Prakash, M. Ahmed, "Hard switching characteristics of SiC and GaN devices for future electric vehicle charging stations," MATEC Web of Conferences, 2021; doi: 10.1051/matecconf/202133502007.

[36] T. Kimoto, J. Cooper, *Fundamentals of Silicon Carbide Technology: Growth, Characterization, Devices and Applications*, 2014, IEEE Press.

[37] G. Messenger, "A summary review of displacement damage from high energy radiation in silicon semiconductors and semiconductor devices," *IEEE Transaction on Nuclear Science*, vol. 39, no. 3, pp. 468-473, 1992, doi: 10.1109/23.277547.

[38] J. Colinge, M. Gao, A. Romano, H. Maes, C. Claeys, "Silicon-on-insulator "gate-all-around" MOS device," IEEE SOS/SOI Technology Conference, 1990, doi: 10.1109/IEDM.1990.237128.

[39] H. Sazawa, A. Nakajima, S. Kuboya, H. Umezawa, T. Kato, Y. Tanaka, "SiC-based high electron mobility transistor," *Applied Physics Letters*, vol. 124, p. 120601, 2024, doi: 10.1063/5.0202925.

[40] M. Lundstrom, *Fundamentals of Carrier Transport*, 2000, Cambridge University Press.

[41] S. Sze, Physics of Semiconductor Devices, 1981, John Wiley & Sons.

[42] R. Quaya, C. Moglestue, V. Palankovski, S. Selberherr, "A temperature dependent model for the saturation velocity in semiconductor materials," Materials Science in Semiconductor Processing, vol. 3, no. 1 pp. 149-155, 2000, doi: 10.1016/S1369-8001(00)00015-9.